

5-1-2004

Interstellar H₃⁺ Line Absorption toward LkH α 101

Sean D. Brittain

Clemson University, sbritt@clemson.edu

Theodore Simon

University of Hawaii

Craig Kulesa

University of Arizona

Terrence W. Rettig

University of Notre Dame

Follow this and additional works at: https://tigerprints.clemson.edu/physastro_pubs

 Part of the [Astrophysics and Astronomy Commons](#)

Recommended Citation

Please use publisher's recommended citation.

This Article is brought to you for free and open access by the Physics and Astronomy at TigerPrints. It has been accepted for inclusion in Publications by an authorized administrator of TigerPrints. For more information, please contact kokeefe@clemson.edu.

INTERSTELLAR H_3^+ LINE ABSORPTION TOWARD LkH α 101

SEAN D. BRITTAI¹

Center for Astrophysics, University of Notre Dame, Notre Dame, IN 46556; sbrittai@nd.edu

THEODORE SIMON¹

Institute for Astronomy, University of Hawaii, 2680 Woodlawn Drive, Honolulu, HI 96822

CRAIG KULESA

University of Arizona, Steward Observatory, 933 North Cherry Avenue, Tucson, AZ 85721

AND

TERRENCE W. RETTIG¹

Center for Astrophysics, University of Notre Dame, Notre Dame, IN 46556

Received 2003 September 3; accepted 2004 January 20

ABSTRACT

We present a detection of three lines of the H_3^+ ion in the near-infrared spectrum of the Herbig Be star LkH α 101. H_3^+ is the principal initiator of gas-phase chemistry in interstellar clouds and can be used to constrain the ionization rate or the path length through interstellar material along the line of sight. Essentially all of the observed H_3^+ column of $(2.2 \pm 0.3) \times 10^{14} \text{ cm}^{-2}$ toward LkH α 101 originates in the same dense, dark cloud; less than 1 mag of the ~ 11 total magnitudes of visual extinction is attributable to diffuse material. Constraints on the density [$1 \times 10^4 \text{ cm}^{-3} < n(\text{H}_2) < 4 \times 10^4 \text{ cm}^{-3}$], along with estimates of distances to the obscuring cloud, imply H_2 ionization rates of $6.7 \times 10^{-17} \text{ s}^{-1} < \zeta < 2.7 \times 10^{-16} \text{ s}^{-1}$. The nondetection of fluorescent H_2 emission at the cloud surface implies that the obscuring dark cloud is located at least 20 pc from LkH α 101 and is therefore decoupled from its evolution. The confirmation of significant H_3^+ in dense material addresses earlier concerns that H_3^+ may originate in diffuse material surrounding dense clouds.

Subject headings: cosmic rays — infrared: ISM — ISM: clouds — ISM: molecules — stars: individual (LkH α 101)

1. INTRODUCTION

The molecular ion H_3^+ plays a special role in the chemistry of interstellar clouds. A by-product of the (cosmic ray) ionization of H_2 , it initiates the diverse gas-phase reactions that form many of the 120+ known molecules in interstellar clouds. H_3^+ is formed by the ionization of H_2 into H_2^+ , followed by the rapid reaction $\text{H}_2^+ + \text{H}_2 \rightarrow \text{H}_3^+ + \text{H}$. It is destroyed by recombination with free electrons and reaction with species that have a larger proton affinity than H_2 . In diffuse clouds electron recombination dominates the destruction of H_3^+ , whereas reaction with CO dominates its destruction in dense clouds. The relative simplicity of the formation and destruction mechanisms of H_3^+ makes it possible, in principle, to derive fundamental physical characteristics of diffuse and dense clouds from its abundance.

H_3^+ was first observed in laboratory spectra by Oka (1980), and nearly a decade later in the upper atmosphere of Jupiter (Drossart et al. 1989). With the advent of more sensitive echelle spectrometers operating at infrared wavelengths on large telescopes, H_3^+ has now been detected in a variety of interstellar environments (Geballe & Oka 1996; McCall et al. 1998, 1999, 2003; Geballe et al. 1999; Goto et al. 2002; Kulesa & Black 2003).

While the molecular physics of H_3^+ is simple, an understanding of the chemistry and abundance of H_3^+ in diffuse

clouds is not well established. Interpretation of H_3^+ abundances in diffuse clouds is complicated by the uncertainty in the rate of H_2 ionization, in the abundances of species that destroy H_3^+ , and especially in the electron recombination rate. McCall (2001) has found that the abundance of H_3^+ in some diffuse clouds is much larger than models predict, and later attributed this discrepancy to an enhanced cosmic-ray ionization rate (McCall et al. 2003).

In contrast, the theoretical picture of the chemistry of H_3^+ in dense clouds is clearer. Its formation depends entirely on the ionization rate of H_2 . Unlike diffuse clouds, the ionization rate in dense clouds is constrained. The rate must be much greater than 10^{-18} s^{-1} to initiate observed gas-phase chemistry, but it cannot exceed $\sim 10^{-16} \text{ s}^{-1}$ to prevent overproduction of atomic hydrogen (Solomon & Werner 1971). The destruction of H_3^+ in dense clouds is also better understood since measurement of the abundance of CO (relative to H_2), its most potent dissociative agent, is possible (Lacy et al. 1994) and the reaction rate of CO with H_3^+ is well established (Anicich & Huntress 1986). In principle, it is possible to determine the path length through a dense cloud or the cosmic-ray ionization rate by measuring the column densities of CO, H_3^+ , and H_2 .

There is, however, some controversy as to whether the H_3^+ observed along lines of sight toward dense clouds actually originates in the dense clouds themselves. Van der Tak & van Dishoeck (2000) point out that more distant dark clouds tend to have larger columns of H_3^+ than do nearby clouds. They conclude that H_3^+ largely resides in the diffuse interstellar medium between distant dense clouds and not necessarily in the dense clouds themselves. If this is correct, the lack of H_3^+ production in dense clouds could significantly alter our picture

¹ Visiting Astronomer at the W. M. Keck Observatory, which is operated as a scientific partnership among the California Institute of Technology, the University of California, and the National Aeronautics and Space Administration. The Observatory was made possible by the generous financial support of the W. M. Keck Foundation.

TABLE 1
JOURNAL OF OBSERVATIONS

Grating/Order	Spectral Grasp (cm^{-1})	Lines	Integration (minutes)	S/N
2002 November 15				
K 36	4662–4729	H ₂ (1, 0) S(1)	4	800
M-Wide 19	2495–2533	H ₃ ⁺ Q(1, 0)	2	300
M-Wide 21	2714–2752	H ₃ ⁺ R(1, 0), R(1, 1) ^u	2	300
2003 March 17				
M-Wide 19	2495–2533	H ₃ ⁺ Q(1, 0)	2	200
M-Wide 21	2714–2752	H ₃ ⁺ R(1, 0), R(1, 1) ^u	2	200

of the thermal and ionization balance in star-forming cloud cores. Resolution of this controversy requires a line of sight that is dominated by dense cloud material in which the extinction, density, and temperature of the cloud (inferred by rovibrational CO observations), H₂ abundance, and radiation field can be measured.

The direction toward the Herbig Be star LkH α 101 (HBC 40; Herbig & Bell 1988) is a good candidate for such a study. LkH α 101 is among the brightest ($m_L = 0.48$) Herbig Be stars and is the illuminating source of the NGC 1579 reflection nebula (Herbig 1971). It lies behind an obscuring cloud and is surrounded by an extended H II region, S222 (Redman et al. 1986). Other clouds lie to the north, south, and southwest. The column density of CO in these clouds ranges from less than 10^{18} up to $5 \times 10^{18} \text{ cm}^{-2}$. Kelly, Rieke, & Campbell (1994) have determined the foreground extinction, $A_V = 11.2^{+0.3}_{-0.7}$ mag, based on a variety of infrared line ratios. Tuthill et al. (2002) have imaged LkH α 101 with an infrared interferometer and found a nearly face-on disk ($i < 35^\circ$). This orientation suggests that the observed extinction is likely due to interstellar rather than circumstellar material. In this work, we present our detection of the Q(1, 0), R(1, 0), and R(1, 1)^u lines of H₃⁺ along the line of sight toward LkH α 101, which serves as a test case that constrains the origin of H₃⁺ in dark clouds.

2. OBSERVATIONS

Absorption spectra of the $v_2 \leftarrow 0$ fundamental lines Q(1, 0), R(1, 0), and R(1, 1)^u of H₃⁺ in the $4 \mu\text{m}$ L'-band atmospheric window were obtained at the W. M. Keck Observatory. We used the cross-dispersed NIRSPEC echelle spectrograph, which provides a spectral resolving power of 25,000 (McLean et al. 1998). The complete set of observations is summarized in Table 1. See Brittain et al. (2003) for a discussion of the data acquisition and reduction procedures.

After a correction for atmospheric absorption, the residual spectral extracts were found to have a fringe with an amplitude of $\sim 1\%$ (Figs. 1 and 2). We removed this fringe by examining the power spectrum and deleting the corresponding frequency spikes from the power spectrum. The defringed segments containing the H₃⁺ lines are displayed in Figures 3 and 4.

3. ANALYSIS

We detected three absorption lines of H₃⁺ along the line of sight toward LkH α 101. Table 2 presents the observed position, rest position, heliocentric radial velocity, equivalent width, and inferred column density for these lines.

LkH α 101 is a rich source of atomic emission lines (Herbig 1971), which may originate from the H II region that surrounds the central star (Redman et al. 1986). Herbig (1971) notes a radial velocity of 8 km s^{-1} for the optical and near-infrared lines of LkH α 101, but with a large scatter. Millimeter observations of CO by Redman et al. (1986) indicate the obscuring cloud in front of the star has a $v_{\text{rad}} = 4.5\text{--}6.3 \text{ km s}^{-1}$, with the peak of the emission at $v_{\text{rad}} = 5.8 \text{ km s}^{-1}$. A CO survey by Ungerechts & Thaddeus (1987) finds the cloud along the line of sight toward LkH α 101 (cloud 12e) is at $v_{\text{rad}} = 6.2 \text{ km s}^{-1}$. In our NIRSPEC spectra of 2002 November and 2003 March, we measure a heliocentric radial velocity for H₃⁺ of 6 ± 1 and $5 \pm 1 \text{ km s}^{-1}$, respectively. The mean radial velocities of the CO emission at submillimeter wavelengths and the H₃⁺ absorption features at infrared wavelengths are consistent, suggesting that they originate from within the same cloud. The uncertainty quoted here for H₃⁺ on each date is the standard deviation of the Doppler shifts measured from the three absorption lines. The H₃⁺ features have a FWHM = $16 \pm 5 \text{ km s}^{-1}$ and thus are marginally resolved at the resolution of NIRSPEC (12 km s^{-1}). We used a

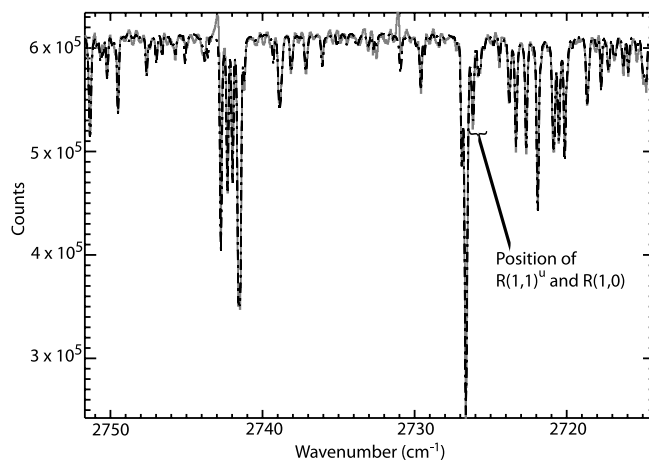


FIG. 1.—Initial (atmospheric and H₃⁺) spectrum and atmospheric model. The two emission features at 2742.8 and 2730.9 cm^{-1} , from H I and O I, result from the surrounding gas. The location of the H₃⁺ lines is indicated. The telluric absorption features dominate the spectrum of LkH α 101. The transmittance function of the night sky was modeled (dashed line) using the Spectrum Synthesis Program (SSP; Kunde & Maguire 1974), which accesses the '92HITRAN molecular database (Rothman et al. 1992). The optimized model establishes the columns of absorbing atmospheric species, the spectral resolving power, and the wavelength calibration. The position of the R(1, 1)^u, R(1, 0) doublet of H₃⁺ is indicated, but further analysis is needed to remove atmospheric and instrumental effects.

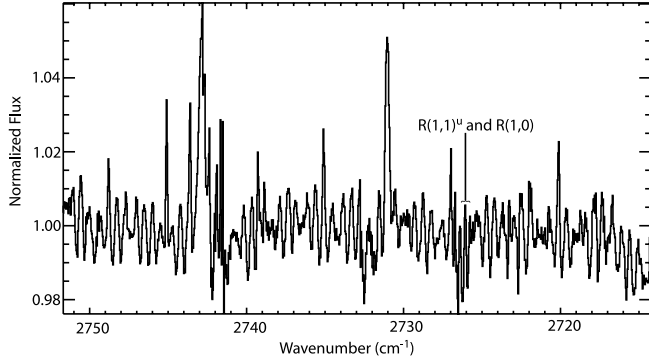


FIG. 2.—Residual spectrum. Division of the observed spectrum by the optimized atmospheric model provides a residual spectrum of absorption and emission lines. The location of the H_3^+ lines is indicated, but the instrumental fringing, having an amplitude of $\sim 1\%$, makes identification difficult.

Gaussian line fit to the profiles to measure their equivalent widths, $W_{\tilde{\nu}}$, and present the results of the fits in Table 2.

From the observed equivalent widths (assumed to be on the linear part of the curve of growth), we computed the column density of gas in the lower molecular levels of each transition by means of the standard relation,

$$W_{\tilde{\nu}} = (8\pi^3 \tilde{\nu} / 3hc) N_{\text{level}} |\mu|^2,$$

where μ is the transition dipole moment (McCall 2001). The level populations inferred for the lower states of the $Q(1, 0)$, $R(1, 0)$, and $R(1, 1)^u$ transitions are listed in Table 2. The $Q(1, 0)$ and $R(1, 0)$ lines probe the same lower state, and the $R(1, 1)^u$ line probes the only other state that can be populated at temperatures of less than a few hundred kelvins. Thus, the total column density of H_3^+ can be calculated from the sum of the $J = 1, K = 0$ state, probed by $Q(1, 0)$ and $R(1, 0)$, and the $J = 1, K = 1$ state, probed by $R(1, 1)^u$. Averaging the level populations for the two nights of observations, we obtain $N(\text{H}_3^+) = (2.2 \pm 0.3) \times 10^{14} \text{ cm}^{-2}$. McCall et al. (1999)

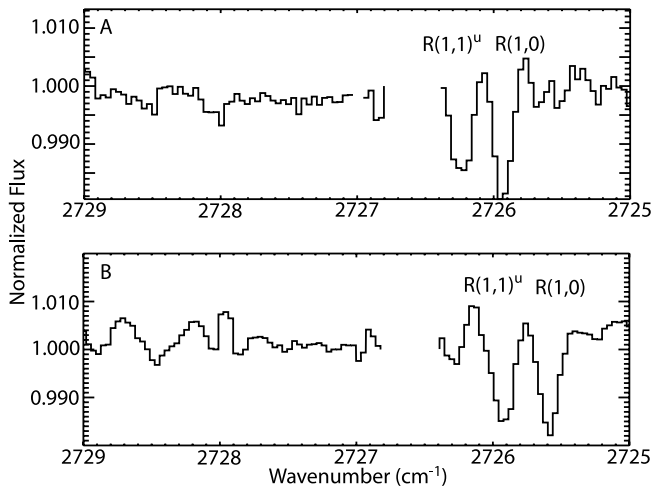


FIG. 3.—Fringe removed from spectra. The instrumental fringe has been removed from the spectra. The fully processed spectral segments (2729–2725 cm^{-1}) observed on (a) 2002 November 15 and (b) 2003 March 17 reveal the H_3^+ $R(1, 1)^u$, $R(1, 0)$ doublet. The shift in position of the lines from (a) to (b) is due to Earth's relative orbital velocity on the two dates, 8.8 and -28.3 km s^{-1} , respectively. The small gaps in the spectra result from incomplete removal of telluric features.

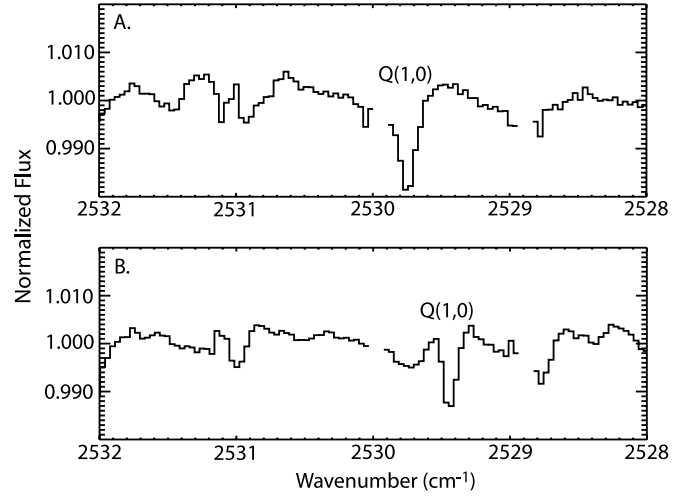


FIG. 4.— H_3^+ spectral lines. The fully processed spectral segments of the H_3^+ $Q(1, 0)$ line observed on (a) 2002 November 15 and (b) 2003 March 17 confirm the detection of the H_3^+ $Q(1, 0)$ line. The relative Doppler shift of this line is consistent with the relative Doppler shift of the H_3^+ doublet.

included LkH α 101 in their H_3^+ survey of dense clouds and derived a 3σ upper limit for the column density of $7 \times 10^{13} \text{ cm}^{-2}$ for the $J = 1, K = 1$ level. It seems likely that systematic uncertainties in the continuum fit and incomplete removal of telluric features may have led to their underestimation of the abundance of H_3^+ toward LkH α 101.

The ortho and para levels of H_3^+ are expected to be thermalized at the local gas temperature through collisional processes and proton exchange with H_2 . The thermalization of these levels has been confirmed for multiple lines of sight through dense clouds for both H_2 (Kulesa & Black 2003) and H_3^+ (McCall et al. 1999). Thus, the ortho/para ratio provides a sensitive and reliable diagnostic of the kinetic temperature of the gas in which H_3^+ is found. The $R(1, 0)$ and $R(1, 1)^u$ doublet probes the ortho as well as para spin modifications of the H_3^+ molecule. The ratio of the strengths of these lines defines the excitation temperature of the gas, according to the Boltzmann formula

$$N_{\text{ortho}}/N_{\text{para}} = (g_{\text{ortho}}/g_{\text{para}}) e^{-\Delta E/kT} = 2e^{-32.87/T}.$$

The excitation temperature we derive from our observations of H_3^+ in 2002 November is $32 \pm 5 \text{ K}$, and that from the data taken in 2003 March is $23 \pm 8 \text{ K}$.

4. CHARACTERIZING THE GASEOUS LINE OF SIGHT TOWARD LkH α 101

4.1. Evidence for a Single Dark Cloud

In order to interpret the presence of H_3^+ line absorption toward LkH α 101, it is first necessary to characterize the nature of the intervening cloud(s), since the chemistry of H_3^+ differs from diffuse to dense clouds. The foreground extinction of LkH α 101 is $A_V = 11.2^{+0.3}_{-0.7} \text{ mag}$ (Kelly et al. 1994). If the ratio of total to selective extinction is normal [i.e., $R_V = A_V/E(B-V) = 3.1$; Cardelli, Clayton, & Mathis 1989], then the column density of gas implied by the empirical relation of Bohlin, Savage, & Drake [1978; $N_{\text{H}}/E(B-V) = 5.5 \times 10^{21} \text{ atoms cm}^{-2} \text{ mag}^{-1}$] is $N_{\text{H}} = 2.2 \times 10^{22} \text{ atoms cm}^{-2}$. If our line of sight passes through a dense cloud, hydrogen is mostly in molecular form, and $N(\text{H}_2) = N_{\text{H}}/2 = 1.1 \times 10^{22} \text{ molecules cm}^{-2}$.

TABLE 2
MEASUREMENTS AND RESULTS FOR H_3^+

Line ID	$\tilde{\nu}_{\text{obs}}$ (cm^{-1})	$\tilde{\nu}_{\text{rest}}$ (cm^{-1})	v_{rad} (km s^{-1})	$W \pm \delta W$ (10^{-3} cm^{-1})	$ \mu ^2$ (D^2)	N_{level} (10^{14} cm^{-2})
2002 November 15						
$Q(1, 0)$	2529.743	2529.724	6.6	2.8 ± 0.3	0.0254	1.0 ± 0.1
$R(1, 0)$	2725.932	2725.898	5.1	2.7 ± 0.3	0.0259	0.9 ± 0.1
$R(1, 1)^u$	2726.238	2726.220	6.9	2.4 ± 0.3	0.0158	1.4 ± 0.2
2003 March 17						
$Q(1, 0)$	2529.441	2529.724	5.3	1.4 ± 0.5	0.0254	0.5 ± 0.2
$R(1, 0)$	2725.587	2725.898	4.2	2.2 ± 0.5	0.0259	0.8 ± 0.3
$R(1, 1)^u$	2725.925	2726.220	6.0	2.3 ± 0.5	0.0158	1.3 ± 0.5

The amount of CO in the foreground gas can be used to determine whether it is consistent with a dense or diffuse cloud environment because the CO abundance varies strongly with environment. The CO/H₂ ratio varies from 1.5×10^{-4} in dark clouds (Kulesa & Black 2003) to as little as 10^{-7} in diffuse clouds exposed to a substantial radiation field (van Dishoeck & Black 1988). Mitchell et al. (1990) observed the 4.7 μm fundamental band of ¹²CO in absorption toward LkH α 101 and derived a CO column density, $N(^{12}\text{CO}) = 1.1 \times 10^{17} \text{ cm}^{-2}$, under the assumption that the lines are optically thin. However, recent work by Goto et al. (2003) provides more sensitive infrared spectroscopy toward LkH α 101, including observations of the ¹³CO fundamental band absorption at 4.7 μm and the ¹²CO overtone absorption lines at 2.3 μm . Those authors note that the ¹²CO fundamental band lines are heavily saturated and find an order of magnitude larger CO abundance, $N(\text{CO}) = (1.84 \pm 0.11) \times 10^{18} \text{ cm}^{-2}$, using the ¹³CO bands and the ¹²CO overtone bands. Thus the CO/H₂ ratio is $\sim 10^{-4}$, typical for a dense cloud. Also, the excitation temperature they find for the ¹³CO lines is 30 K, which is indicative of cold, dense cloud material and consistent with the temperature we derive for H₃⁺.

We have computed a suite of cloud models based on work by van Dishoeck & Black (1986, 1988), which calculate the abundances of important species such as H, H₂, C⁺, C, and CO as a function of depth into a cloud. Figure 5 demonstrates the depth dependence of the hydrogen- and carbon-bearing species for one interstellar cloud model appropriate to LkH α 101, a dense cloud with $n_{\text{H}} = 10^4 \text{ cm}^{-3}$ in a uniform $2.2 \times$ Habing ($I_{\text{UV}} = 1$) radiation field.² The integrated column densities from this model provide $A_V = 11$ – 13 mag and account for all of the observed CO. The 3σ upperlimit for the extinction toward LkH α 101 is $A_V \sim 12$ (Kelly et al. 1994); thus we find that at most 1 mag of diffuse material is warranted for this line of sight. Therefore, $N_{\text{H}} < 2 \times 10^{21} \text{ cm}^{-2}$ for a typical diffuse cloud gas-to-dust ratio (Bohlin et al. 1978).

Can a diffuse cloud that provides ~ 1 mag of visual extinction contain the observed H₃⁺? For a typical diffuse cloud, $N(\text{H}_3^+) = [\zeta L N(\text{H}_2)] / [k_e N(e^-)]$ (McCall et al. 2003), so that $\zeta L = [k_e N(e^-) N(\text{H}_3^+)] / N(\text{H}_2)$, where ζ is the ionization rate of H₂, L is the path length through the cloud, and k_e is the electron recombination rate, $2 \times 10^{-7} \text{ cm}^3 \text{ s}^{-1}$ (McCall et al. 2003). We adopt $N(e^-) \sim 5 \times 10^{17} \text{ cm}^{-2}$ if all elemental

carbon (C/H $\sim 2.4 \times 10^{-4}$; Cardelli et al. 1996) is singly ionized, assuming that L is not larger than a few parsecs. The resulting ionization rate, $\zeta > 10^{-14} \text{ s}^{-1}$, has profound consequences for the dense cloud. The ionization would increase the atomic hydrogen fraction to nearly 10^{-1} , but observations by Dewdney & Roger (1982) show that cold atomic hydrogen in 21 cm absorption toward LkH α 101 contributes only 10^{-2} of the total hydrogen.

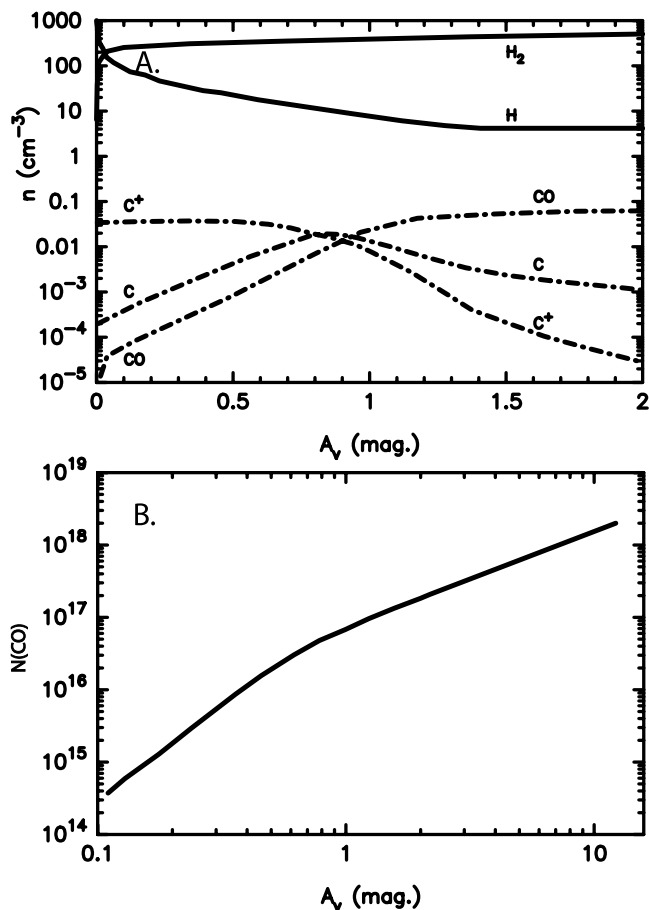


FIG. 5.—Cloud models. (a) Depth dependence of the hydrogen- and carbon-bearing species for one interstellar cloud model appropriate to LkH α 101: an interstellar cloud with $n_{\text{H}} = 10^4 \text{ cm}^{-3}$ in a uniform $2.2 \times$ Habing ($I_{\text{UV}} = 1$) radiation field. (b) Cumulative column density of CO is plotted as a function of increasing depth into the dense cloud.

² $I_{\text{UV}} = 1$ corresponds to an integrated intensity of 912–1130 Å photons of $4.76 \times 10^{-5} \text{ ergs s}^{-1} \text{ cm}^{-2} \text{ sr}^{-1}$.

If we consider the limiting case in which all production of atomic hydrogen is governed by cosmic-ray ionization and balanced by the formation of molecular hydrogen at the Jura (1974) rate, then $\zeta < 10^{-15} \text{ s}^{-1}$. This is a strong upper limit because efficient dissociation of H₂ by UV radiation has been entirely neglected. Even if the cosmic-ray power spectrum is dominated by low-energy particles incapable of penetrating dark clouds, the high ionization rate measured by McCall et al. (2003) toward the diffuse cloud around ζ Per only manages to produce a small fraction (~10%) of the observed H₃⁺ toward LkHα 101. It is also important to note that the temperature of H₃⁺ that we observe, ~30 K, is identical to the rotational temperature of the dark cloud CO observed in absorption (Goto et al. 2003) and significantly lower than the 70–1200 K spin temperature of the diffuse H I emission observed by Dewdney & Roger (1982). We conclude that most of the observed H₃⁺ originates in the dense material, although a small fraction of the H₃⁺ may reside in warmer diffuse material along the line of sight.

4.2. Location of the Cloud along the Line of Sight

The distance to LkHα 101 is uncertain. It has been estimated to be 160 pc by Stine & O’Neil (1998), 350 pc by Ungerechts & Thaddeus (1987), and at least 800 pc by Herbig (1971). Redman et al. (1986) suggest that the obscuring cloud is not intimately associated with LkHα 101, but this does not tightly constrain the cloud’s location. A tighter constraint on the proximity of the cloud is provided by the upper limit on the H₂ features in our 2 μm spectroscopy. If the cloud is close to the star, a significant nonionizing UV continuum and Lyα flux from LkHα 101 should lead to measurable H₂ fluorescence from the surface of the cloud. We measure an upper limit of the H₂ (1–0) S(1) line emission at 4712.9 cm⁻¹ (2.1218 μm) of 10⁻⁷ ergs s⁻¹ cm⁻² sr⁻¹, which limits exposure of H₂ within the intervening cloud to a radiation field of $I_{UV} \ll 1$. We interpolate the ATLAS 9 (Kurucz 1993) and CoStar models (Schaerer et al. 1996) to estimate the specific luminosity of H₂-fluorescing photons from a 24,000 K star: 2.7×10^{32} photons s⁻¹. The distance from LkHα 101 at which this ultraviolet radiation field would be quenched to $I_{UV} \ll 1$ is at least 20 pc.

4.3. The H₃⁺ Abundance and Ionization Rate in Dense Molecular Environments

Our characterization of the gaseous environment toward LkHα 101 constrains our physical interpretation of H₃⁺ line absorption. H₃⁺ is a unique molecule in that, to first order, its number density is independent of the total number density of the dense cloud (McCall et al. 1998). The formation rate of H₃⁺ is determined by the ionization rate of H₂, ζ, which is dominated by cosmic rays. The rate can be enhanced by a local X-ray radiation field such as that produced by a young star or group of stars that form in such environments (Black 2000). In a dense cloud, the destruction of H₃⁺ is dominated by reaction with CO, whose reaction rate is $k_{CO} = 2 \times 10^{-9} \text{ cm}^3 \text{ s}^{-1}$. Disregarding any other species that can react with H₃⁺ places a lower limit on the cosmic-ray ionization rate of H₂ that is needed to maintain a steady state solution, $\zeta n(\text{H}_2) =$

$k_{CO}n(\text{CO})n(\text{H}_3^+)$, so that $n(\text{H}_3^+) = [\zeta n(\text{H}_2)]/[k_{CO}n(\text{CO})]$. This can be rewritten as

$$\zeta L = k_{CO}N(\text{CO})N(\text{H}_3^+)/N(\text{H}_2).$$

Adopting $N(\text{H}_3^+) = 2.2 \times 10^{14} \text{ cm}^{-2}$ from § 3, $N(\text{H}_2) = 1.1 \times 10^{22} \text{ cm}^{-2}$ and $N(\text{CO}) = 2 \times 10^{18} \text{ cm}^{-2}$ from § 4.1, we find $\zeta L = 80 \text{ cm s}^{-1}$.

The angular extent of the obscuring cloud in the plane of the sky is 2' (Redman et al. 1986). The physical dimension of the cloud depends on its distance, and our only constraint is that it be at least 20 pc from LkHα 101. At the distances mentioned earlier, $d = 160, 350,$ and 800 pc , the path length through the cloud is 0.09, 0.2, and 0.4 pc, respectively, assuming that it is spherical. The implied gas densities, $n(\text{H}_2) = N(\text{H}_2)/L$, are $4 \times 10^4, 2 \times 10^4,$ and $1 \times 10^4 \text{ cm}^{-3}$. These are consistent with the firm upper limit of $2 \times 10^5 \text{ cm}^{-3}$ that we find from a detailed analysis of the infrared CO absorption lines (C. A. Kulesa et al. 2004, in preparation). The resulting ionization rate indicated for each distance is $3 \times 10^{-16}, 1.3 \times 10^{-16},$ and $6.7 \times 10^{-17} \text{ s}^{-1}$.

These derived ionization rates are lower limits, since we neglect other destructive species. In particular, O/CO ranges from ~0.5 to 1, and $k_O/k_{CO} \sim 0.5$. Thus the ionization rate can be enhanced by as much as 50%. If the dark cloud is at 800 pc, preferred by Herbig (1971), then the observed ionization rate of the H₂ is consistent with the constraints determined by Solomon & Werner (1971). No sources of local ionization can explain the larger derived ionization rates at the nearer cloud distances. The only possible local source of ionization is a cluster of T Tauri stars located 0.5–2' from the line of sight toward LkHα 101, at a distance of 160 pc. Following the treatment of Maloney, Hollenbach, & Tielens (1996), we derive a maximal local ionization enhancement of only $1.2 \times 10^{-17} \text{ s}^{-1}$ for an X-ray luminosity of $10^{32} \text{ ergs s}^{-1}$ and the minimum projected star-cloud distance of 0.1 pc. The derived ionization rate is therefore dominated by cosmic rays and not by a local enhancement to the radiation field. The cosmic-ray ionization rate will be better constrained once the gas density or the relationship of the obscuring cloud and LkHα 101 can be better established.

5. CONCLUSION

We have presented observations of H₃⁺ absorption toward LkHα 101. The study of this relatively simple line of sight allows the interstellar material to be studied unambiguously. Our upper limit on the column of diffuse material is insufficient to account for the quantity of observed H₃⁺; thus most of the H₃⁺ must originate in a dense cloud. Furthermore, the spin temperature of the H₃⁺ (~30 K) is consistent with the same cold dense gas probed by CO. The identification of H₃⁺ in the obscuring cloud toward LkHα 101 supports the previous attribution of significant H₃⁺ absorption to dense cloud material (McCall 2001).

We thank G. Herbig and S. Andrews for helpful discussions and M. Goto for providing us with a preprint of her CO paper. S. D. B. and T. W. R. were supported for this work under NSF Astronomy grant 02-05881.

REFERENCES

- Anicich, V. G., & Huntress, W. T. 1986, ApJS, 62, 553
 Black, J. H. 2000, Philos. Trans. R. Soc. London A, 358, 2515
 Bohlin, R. C., Savage, B. D., & Drake, J. F. 1978, ApJ, 224, 132
 Brittain, S. D., Rettig, T. W., Simon, T., Kulesa, C., DiSanti, M. A., & Dello Russo, N. 2003, ApJ, 588, 535
 Cardelli, J. A., Clayton, G. C., & Mathis, J. S. 1989, ApJ, 345, 245

- Cardelli, J. A., Meyer, D. M., Jura, M., & Savage, B. D. 1996, *ApJ*, 467, 334
Dewdney, P. E., & Roger, R. S. 1982, *ApJ*, 255, 564
Drossart, P., et al. 1989, *Nature*, 340, 539
Geballe, T. R., McCall, B. J., Hinkle, K. H., & Oka, T. 1999, *ApJ*, 510, 251
Geballe, T. R., & Oka, T. 1996, *Nature*, 384, 334
Goto, M., McCall, B. J., Geballe, T. R., Usuda, T., Kobayashi, N., Terada, H., & Oka, T. 2002, *PASJ*, 54, 951
Goto, M., et al. 2003, *ApJ*, 598, 1038
Jura, M. 1974, *ApJ*, 191, 375
Lacy, J. H., Knacke, R., Geballe, T. R., & Tokunaga, A. T. 1994, *ApJ*, 428, L69
Herbig, G. H. 1971, *ApJ*, 169, 537
Herbig, G. H., & Bell, K. R. 1988, *Lick Obs. Bull.* 1111
Kelly, D. M., Rieke, G. H., & Campbell, B. 1994, *ApJ*, 425, 231
Kulesa, C. A., & Black, J. H. 2003, in *Chemistry as a Diagnostic of Star Formation*, ed. M. Fich & C. L. Curry (Ottawa: NRC Research Press), 60
Kunde, V. R., & Maguire, W. C. 1974, *J. Quant. Spectrosc. Radiat. Transfer*, 14, 803
Kurucz, R. 1993, CD-ROM 13, ATLAS 9 Stellar Atmosphere Programs and 2 km/s Grid (Cambridge: SAO)
Maloney, P. R., Hollenbach, D. J., & Tielens, A. G. G. M. 1996, *ApJ*, 466, 561
McCall, B. J. 2001, Ph.D. thesis, Univ. Chicago
McCall, B. J., Geballe, T. R., Hinkle, K. H., & Oka, T. 1998, *Science*, 279, 1910
———. 1999, *ApJ*, 522, 338
McCall, B. J., et al. 2003, *Nature*, 422, 500
McLean, I. S., et al. 1998, *Proc. SPIE*, 3354, 566
Mitchell, G. F., Maillard, J. P., Allen, M., Beer, R., & Belcourt, K. 1990, *ApJ*, 363, 554
Oka, T. 1980, *Phys. Rev. Lett.*, 45, 531
Redman, R. O., Kuiper, T. B. H., Lorre, J. J., & Gunn, J. E. 1986, *ApJ*, 303, 300
Rothman, L. S., et al. 1992, *J. Quant. Spectrosc. Radiat. Transfer*, 48, 469
Schaerer, D., de Koter, A., Schmutz, W., & Maeder, A. 1996, *A&A*, 310, 837
Solomon, P. M., & Werner, M. W. 1971, *ApJ*, 165, 41
Stine, P. C., & O'Neal, D. 1998, *AJ*, 116, 890
Tuthill, P. G., Monnier, J. D., Danchi, W. C., Hale, D. D. S., & Townes, C. H. 2002, *ApJ*, 577, 826
Ungerechts, H., & Thaddeus, P. 1987, *ApJS*, 63, 645
van der Tak, F. F. S., & van Dishoeck, E. F. 2000, *A&A*, 358, L79
van Dishoeck, E. F., & Black, J. H. 1986, *ApJS*, 62, 109
———. 1988, *ApJ*, 334, 771